Journal of Hydrology, 136 (1992) 333–352
Elsevier Science Publishers B.V., Amsterdam

[2]

Quantitative assessment of the flow pattern in the southern Arava Valley (Israel) by environmental tracers and a mixing cell model

E.M. Adar[a], E. Rosenthal[b], A.S. Issar[a] and O. Batelaan[c]

[a]*Jacob Blaustein Institute for Desert Research and Department of Geology, Ben-Gurion University of the Negev, Sede-Boqer Campus, 84993, Israel*
[b]*Hydrological Service of Israel, Research Division, P.O.B. 6381, Jerusalem 91063, Israel*
[c]*Vrije Universitet, Institut voor Aardwetenschappen, Postbus 7161, Amsterdam 1007 MC, Netherlands*

(Received 6 July 1991; accepted 2 November 1991)

ABSTRACT

Adar, E.M., Rosenthal, E., Issar, A.S. and Batelaan, O., 1992. Quantitative assessment of the flow pattern in the southern Arava Valley (Israel) by environmental tracers and a mixing cell model. J. Hydrol., 136: 333–352.

This paper demonstrates the implementation of a novel mathematical model to quantify subsurface inflows from various sources into the arid alluvial basin of the southern Arava Valley divided between Israel and Jordan. The model is based on spatial distribution of environmental tracers and is aimed for use on basins with complex hydrogeological structure and/or with scarce physical hydrologic information. However, a sufficient qualified number of wells and springs are required to allow water sampling for chemical and isotopic analyses. Environmental tracers are used in a multivariable cluster analysis to define potential sources of recharge, and also to delimit homogeneous mixing compartments within the modeled aquifer. Six mixing cells were identified based on 13 constituents. A quantitative assessment of 11 significant subsurface inflows was obtained. Results revealed that the total recharge into the southern Arava basin is around 12.52×10^6 m^3 year^{-1}. The major source of inflow into the alluvial aquifer is from the Nubian sandstone aquifer which comprises 65–75% of the total recharge. Only 19–24% of the recharge, but the most important source of fresh water, originates over the eastern Jordanian mountains and alluvial fans.

INTRODUCTION

The southern Arava Valley is a narrow downfaulted rift valley, about 20 km, wide extending about 80 km north of the Gulf of Elat (Fig. 1). It is an extremely arid basin with average annual precipitation of about 50 mm. Owing to its geological and geophysical nature, the rift forms a low base level into which surface as well as subsurface flows drain from the surrounding highlands. The

Correspondence to: E.M. Adar, Jacob Blaustein Institute for Desert Research and Department of Geology, Ben-Gurion University of the Negev, Sede-Boqer Campus, 84993, Israel.

0022-1694/92/$05.00 © 1992 — Elsevier Science Publishers B.V. All rights reserved

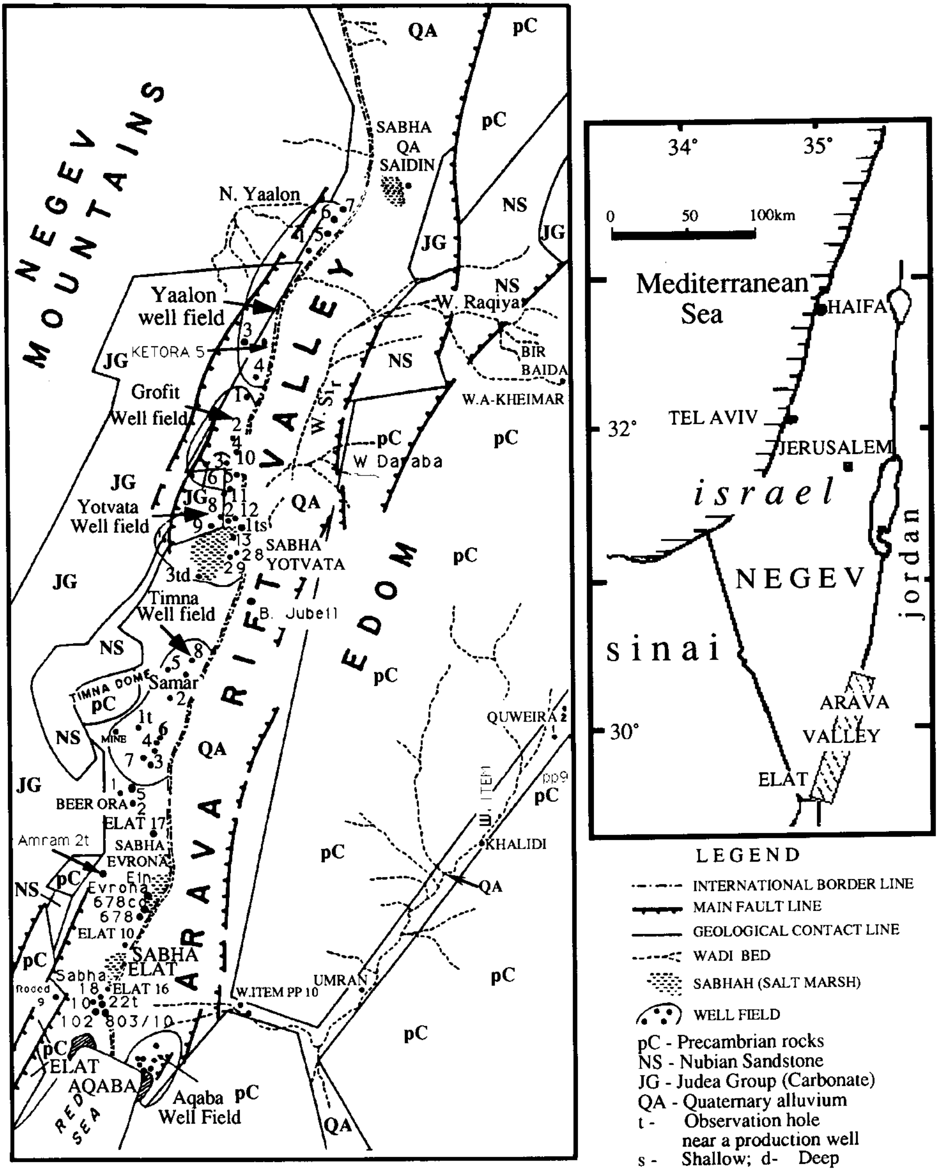

Fig. 1. Map of the southern Arava basin showing the location of main well fields and a schematic depiction of major geological units.

aquifers bordering the valley are (from bottom to top): (1) sandstones of Paleozoic age; (2) sandstones of Lower Cretaceous age; (3) limestone of Cretaceous age; (4) alluvial fill of Quaternary age. Because of the extremely complex geologic structures caused by tilted faults followed by upward and/or downward movement of blocks, it is almost impossible to obtain detailed and reliable information on the physical and hydrogeological properties of each structural component of the aquifer system. Hence, at this stage a quantitative assessment of the flow system by numerical modeling is not possible.

The aim of this study was to differentiate and evaluate the contribution of each aquifer and to quantify every subsurface source of inflow into the alluvial aquifer within the southern Arava rift valley. For this, we used a mathematical model which utilizes environmental isotopes and dissolved minerals. This model was originally developed for the Aravaipa Valley, a small arid basin in Arizona (Adar and Neuman, 1988; Adar et al., 1988), while in this paper we present results from a revised mathematical algorithm. This enabled us to deal with a bigger and more complex hydrogeologic system, such as the Arava rift valley and to obtain a quantitative assessment of recharge sources. The results, however, apply only to the southern Arava basin along 80 km north of the Gulf of Elat (Fig. 1).

Complete chemical and isotopic analyses of 369 water samples from the southern Arava basin were interpreted by means of mixing and composite diagrams and by multivariable factor and cluster analyses (Batelaan, 1989; Rosenthal et al., 1990). Ward's agglomeration method (Norusis, 1985) was used for clustering and the output is displayed in a form of dendograms. With this method all variables are given an equal weight for the calculation of relative closeness for the quantitative definition of discrete water bodies (Everit, 1980). Results are presented as relative distances on a scale of 0–25. Twenty distinguishable groups of water were identified including six groups which are located along the alluvial valley. The final clustering based on Ward's method, which identified groups of potential groundwater sources and the discretization of the aquifer into six cells, is presented as dendograms in Fig. 2. Similar results were also obtained with the centroid clustering method (Batelaan, 1989).

The wells which comprise each group of potential inflows are listed in Table 1. The wells which comprise each cell and the associated chemical and isotopic values are given in Table 2. The chemical and isotopic characteristics of the potential inflows are given in Table 3.

The cluster analyses and the data presented in Table 1 demonstrate that many wells drilled into certain formations, actually extract water originating from a different water-bearing layer which has flowed into it owing to the aforementioned complex hydrogeological structure.

Results from cluster analyses and the spatial distribution of conservative tracers such as oxygen-18 and deuterium suggested the subsurface flow pattern presented in Fig. 3. The processed hydrochemical and isotopic

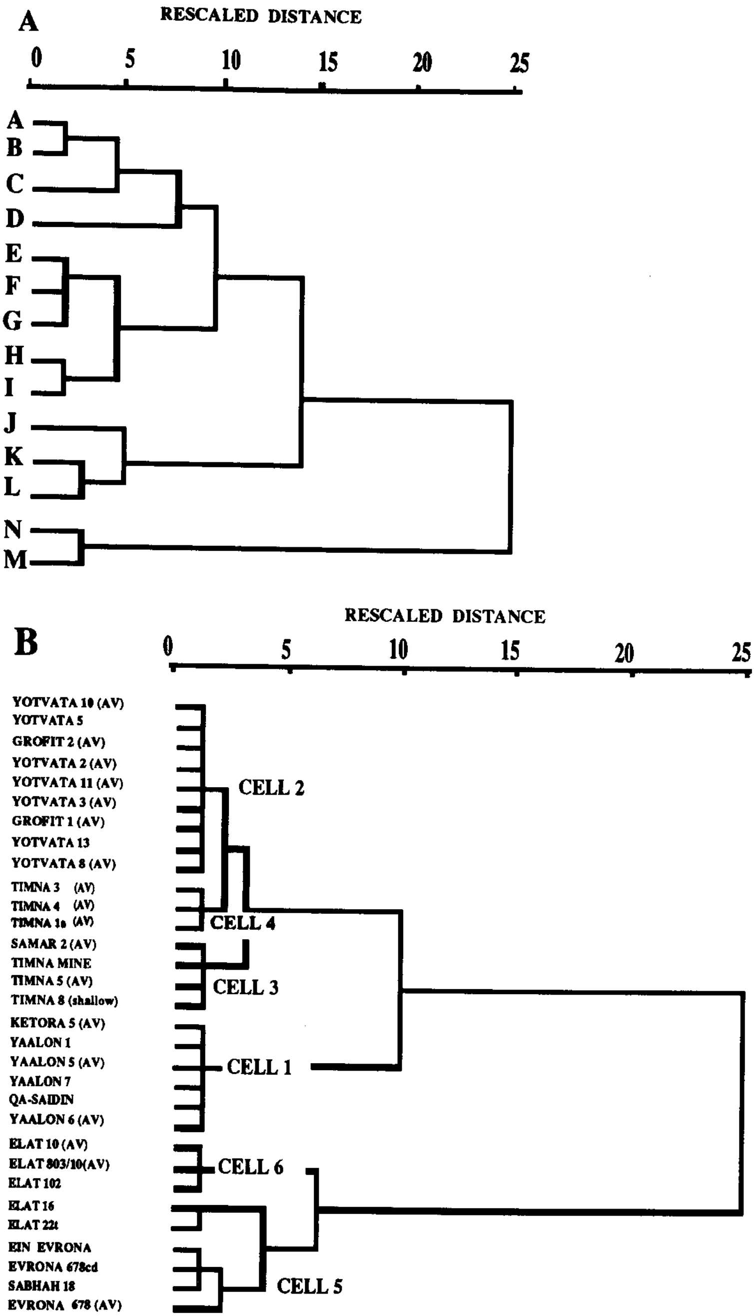

Fig. 2. Dendogram of: (A) a cluster analysis showing the potential sources of, and the possible relations (mixing) between, cell units; (B) a cluster analysis showing the partitioning of the alluvial aquifer into six mixing cells.

TABLE 1

List of wells and the water-bearing formations comprising each subcluster as obtained by a multivariables cluster analysis and presented in Fig. 2

Sub-cluster	Loc.	Geo.	Loc.	Geo.	Loc.	Geo.	Loc.	Geo.	Loc.	Geo.	Loc.	Geo.
A	AMRAM 2T	All.	ELAT 10	All.	ELAT 803/10	All.						
B	ELAT 16	All.	SABHAH 18	All.								
C	GROFIT 3	Kur.	TIMNA 2	All.	TIMNA 6	All.	YOTVATA SABHA (29)	All.				
D	BEER ORA 5	Jud.	TIMNA 8 (DEEP)	All.	YOTVATA SABHA (28)	All.						
E	BEER ORA 1	Jud.	TIMNA 3	All.	TIMNA 4	All.	YOTVATA 1t	All.	YOTVATA 3t DEEP	All.		
F	YOTVATA 2	Jud.	YOTVATA 12t	Kur.	YOTVATA 12	Kur.						
G	GROFIT 2	Jud.	YOTVATA 2	Jud.	YOTVATA 13	Jud.	YOTVATA 10	Jud.	YOTVATA 11	Jud.	YOTVATA 13	All.
H	NAKHEL[a] DEEP		YAALON 3	Kur.	YAALON 4	Kur.	YOTVATA 9t	Kur.				
I	SAMAR 2	All.	TIMNA 5	All.	TIMNA 7	All.	TIMNA 8 (shallow)	All.	TIMNA[c] 161 (shallow)	Kur.		
J	QUWEIRA[b] PP9	Kur.	RAM[b] spring	Kur.	QA-DISI[b] S2	Kur.	SA.ESSWAN[b] S3	Kur.	QA-KHREIM[b] S4	Kur.	QU-WEIRA[b] S5	Kur.
	QA-GHAL[b] S7	Kur.	QA-DISI2[b] S19	Kur.	QA-DISI3[b] S22	Kur.	W.MJHEIS[b] S36	Kur.	HLSWA[b] S49	Kur.		
K	BAIDA SP.	Kur.	KETORA 5	Kur.	YAALON 5	Kur.	YAALON 6	Kur.				
L	YAALON 1	Kur.	YOTVATA 9	Jud.								
M	TIMNA[c] FB178	Kur.	TIMNA[c] FB181	Kur.	TIMNA[c] FB182	Kur.						
N	TIMNA[c] FA248	Kur.	TIMNA[c] SL162	Kur.								

[a]Central Sinai, not shown in Fig. 1.
[b]Southeast Jordan, not shown in Fig. 1.
[c]Timna mine area; observation holes not shown in Fig. 1.
Loc, location; Geo., formation tapped by well; All., alluvium; Kur., Kurnub Sandstone Formation; Jud., Judea limestone; t, observation well near the listed well.

TABLE 2

Average ionic concentrations and isotopic ratios of ground water within each cell

Cell	Wells		TDI ($mEq\ l^{-1}$)	HCO_3 ($mEq\ l^{-1}$)	SO_4 ($mEq\ l^{-1}$)	Cl ($mEq\ l^{-1}$)	Ca ($mEq\ l^{-1}$)	Mg ($mEq\ l^{-1}$)	Na + K ($mEq\ l^{-1}$)	O^{18} (‰ vs. SMOW)	D (‰ vs. SMOW)
1	Yaalon 1, 5, 6, 7	Avg.	42.59	4.18	6.89	10.17	6.52	6.44	8.36	−5.50	−27.9
	Qa Saidin	SD	7.52	0.28	2.00	2.07	1.31	1.05	1.64	1.02	–
	Ketora 5										
2	Grofit 1, 2	Avg.	74.33	4.22	17.62	15.25	12.15	11.86	13.1	−6.27	−40.9
	Yotvata 2, 3, 5	SD	5.28	0.27	1.03	1.79	1.27	0.93	1.4	0.18	2.38
	8, 1O, 11, 13										
3	Samar 2, Timna 5	Avg.	105.7	3.69	9.64	29.50	19.79	11.97	21.14	−7.63	−53.0
	Timna 8S	SD	3.74	0.23	2.29	2.46	1.349	0.33	0.75	0.21	4.8
	Timna mine										
4	Timna 13, 4	Avg.	80.79	3.21	15.6	21.54	12.64	11.38	16.39	−6.45	−43.0
		SD	1.635	0.92	0.70	0.55	0.57	0.45	0.18	–	–
5	Evrona 678C/d, 678 A										
	Ein Evrona	Avg.	135.08	2.05	16.3	48.91	22.67	14.13	30.98	−6.10	−35.6
	Sabhah 18	SD	13.58	0.88	2.4	4.98	5.7	2.46	2.66	–	–
6	Elat 1O, 16,	Avg.	202.99	1.31	19.6	80.49	33.75	20.17	47.32	−6.79	−45.1
	803/10, 102, 22t	SD	19.74	0.23	2.6	7.44	3.52	6.05	5.71	0.58	10.3

Avg., average; SD, standard deviation; TDI, total dissolved ions; SMOW, standard mean oceanic water.

TABLE 3

Chemical composition (mEq l^{-1}) of potential sources to each cell

Cell	Wells	TDI[a]	HCO_3	SO_4	Cl	Ca	Mg	Na + K	O^{18b}	D^b
1	Bir Baida	26.58	3.72	3.85	5.50	4.22	3.91	5.38	−5.76	−31.5
	Baagebul[c]	178.7	9.31	0.20	79.6	36.0	12.0	8.36	–	–
	Yaalon 3/4	56.43	3.77	10.24	14.2	9.58	7.15	11.5	−7.65	−50.15
2	Yotvata 12	105.8	4.09	21.5	27.6	15.5	17.1	20.3	−6.58	−35.95
	Yotvata 9	81.96	3.60	20.3	19.5	15.2	10.5	17.9	−4.20	−28.10
	Yotvata 9t	81.08	3.70	13.6	23.5	13.3	9.99	16.9	−7.8	−46.70
3	Baagebul[c]	178.7	9.31	0.20	79.6	36.0	12.0	8.36	–	–
	Yotvata 9t	81.08	3.70	13.6	23.5	13.3	9.99	16.9	−7.8	−46.70
4	Yotvata 9t	81.08	3.70	13.6	23.5	13.3	9.99	16.9	−7.8	−46.70
	Beer Ora 1, 2	72.81	2.94	28.1	6.03	15.8	13.5	6.91	−6.25	−38.00
	Bir Jubeil	174.5	9.31	0.20	79.6	33.6	12.0	39.8	–	–
	Timna 6	196.8	1.84	17.7	78.8	45.9	9.17	43.3	−7.04	−49.40
5	Beer Ora 1, 2	72.81	2.94	28.1	6.03	15.8	13.5	6.91	−6.25	−38.00
	Yaalon 3	82.70	0.49	17.1	23.7	7.79	13.8	19.8	−7.85	−50.00
	Bir Jubeil	174.5	9.31	0.20	79.6	33.6	12.0	39.8	–	–
6	Roded 9	324.7	0.93	17.8	142.8	45.5	28.5	88.8	–	–
	Yaalon 3	82.70	0.49	17.1	23.7	7.79	13.8	19.8	−7.85	−50.00

[a]Total dissolved ions (mEq l^{-1}).
[b]Oxygen-18 and deuterium (‰). Stable isotopes data were not available for all potential contributors.
[c]Southwest Jordan; not shown in Fig. 1.

information was then combined with groundwater level analyses to establish a schematic qualitative potential flow configuration for the southern Arava basin (Fig. 8, Rosenthal et al., 1990). This showed that the alluvial aquifer is recharged from four major sources: (1) lateral subsurface flow originating from infiltration and deep percolation of water from floods generated in the neighboring mountains, and over adjacent alluvial fans; (2) lateral groundwater flow from carbonate formations along the western margins; (3) lateral flows and upward leakage from the Nubian sandstone aquifers; and (4) leakage from deep-seated aquifers containing brine. For the last 15 years or so the inflows are mainly balanced by pumping. Upward leakage into the sabhahs where it is later evaporated, is an important factor in the Yotvata and Evrona sections (Fig. 1). In the southernmost part of the area, near Elat, direct outflow to the Red Sea should be considered, although because of the

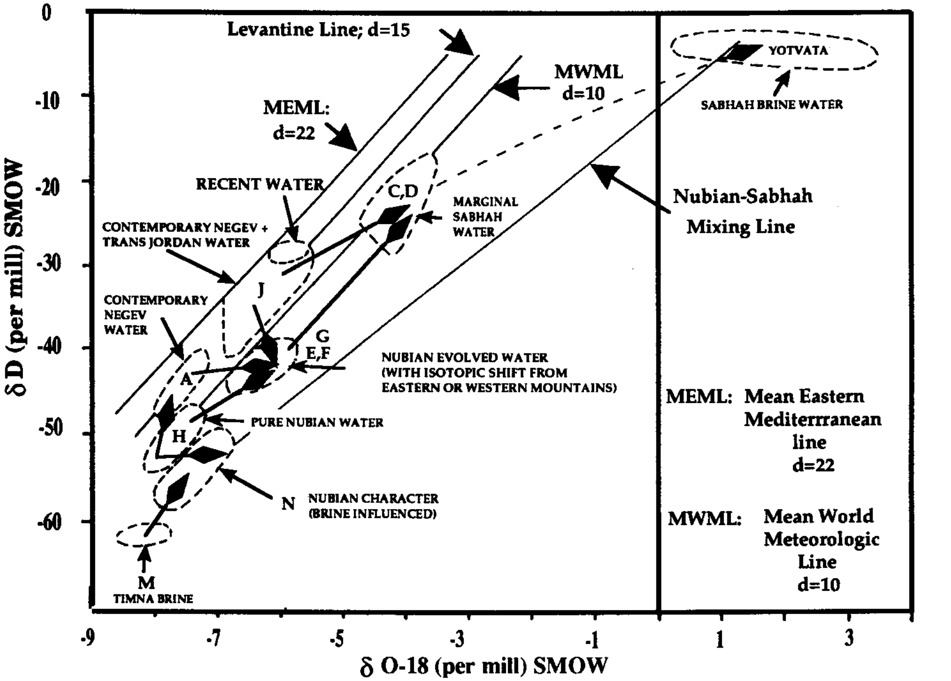

Fig. 3. Schematic flow configuration and relation between groups of water based on cluster analysis presented for oxygen-18 and deuterium. Letters represent subclusters listed in Table 1.

intensive pumping during the last 20 years, this discharge is probably very small. Direct recharge from local rainfall is excluded due to the limited amount of precipitation and high rates of evaporation. No indications were found for deep percolation from floods inside the valley into underlying deep alluvial horizons, as only very extreme floods may reach the lower valley along a very short section. The limited infiltration is quantitatively insignificant and may only recharge the shallow gravel beds from which water is extracted by evapotranspiration.

Constant rate of pumping, water levels and piezometric distribution during the last 15 years suggest a steady flow system in the alluvial aquifer (Rosenthal et al., 1990). In the following sections the same hydrochemical and isotopic data that were used for the qualitative assessment of the flow system will be incorporated into mathematical algorithms for quantitative assessment of recharge from various sources into the southern Arava alluvial aquifer.

THEORY OF QUANTIFICATION OF RECHARGE SOURCES BY A COMPARTMENTAL MIXING CELL MODEL

A model for a quantitative assessment of recharge into an alluvial arid basin using a mixing cell approach was originally presented by Simpson and Duckstien (1976). Campana and Simpson (1984) used the mixing cell approach with carbon-14 data in a discrete-state compartment model for the evaluation of groundwater recharge into the Tucson basin (Arizona, USA). Kirk and Campana (1990) used deuterium as a conservative tracer in a discrete-state mixing cell model to elaborate on the flow system in a complicated basin with scarce hydrogeological data. The above-mentioned model requires an initial estimate of the flow system and a knowledge of the spatial distribution of one environmental tracer over the modeled basin. For any given cell, the state of the cell's concentration is expressed by a weighted mixing of the dissolved species transported across the cell boundaries. Assuming a conservation of mass, recharge values (flows across cell boundaries) are estimated by an iterating process which calibrates water fluxes to the observed concentrations. Discrete-state compartment models which rely on one tracer can not yield a unique solution, and are much dependent on the set-up of the flow system. Herein, we utilize the mixing cell concept but with a multitracer approach to assess a more reliable solution.

The mathematical model employed in the present study was originally developed by Adar et al. (1988) for a small arid basin in Arizona, and was further developed for non-steady seasonal fluctuations by Adar and Sorek (1989). It uses hydrochemical and isotopic data to calculate fluxes of recharge into a complex alluvial aquifer. The model is based on the following assumptions:

(1) The alluvial aquifer can be divided into homogeneous cells in one-, two- or three-dimensional flow patterns. This implies that for every environmental tracer, a unique value can be assigned for each cell.

(2) All water bodies derived from various sources entering the cell mix instantly so that the spatial distributions of the dissolved constituents within each cell are uniform. This approach confirms the mixing cell model as suggested by Campana and Simpson (1984). Hence, neither head nor tracer gradients are allowed within the compartment, except at the cell boundaries.

(3) All tracers are assumed to be reasonably conservative within the flow domain and along the flow path. Fast dissolution or precipitation of minerals is assumed to be negligible.

For the solution, the aquifer is divided into N discrete homogeneous compartments. This is basically a discretization of the flow domain based on hydrogeologic considerations together with multitracer cluster analyses.

Assuming that I_n potential inflows and J_n outflows are identified across the active boundaries of cell n, a water balance expression for cell n can be written as:

$$\sum_{i=1}^{In} q_{in} - Pm_n - \sum_{j=1}^{Jn} q_{nj} = S_n^* \frac{dh_n}{dt} \tag{1}$$

where q_{in} and q_{nj} denote fluxes during dt from the ith source into cell n and from cell n into cell j, respectively. Pm_n and S_n^* designate rate of pumping and storage capacity in cell n. h_n denotes the average hydraulic head which is associated with that compartment for the time interval dt. For a steady flow system or even for an aquifer with periodic seasonal fluctuations (quasi-steady flow), one may identify a time period $\tau = t_2 - t_1$ for which $h_{t=1}$ equals $h_{t=2}$. Thus, S_n is not a function of time ($S_n \neq S_n(t)$), so by integrating eqn. (1) over period τ and dividing by τ, one obtains:

$$\sum_{i=1}^{I_n} Q_{in} - \sum_{j=1}^{J_n} Q_{nj} - \overline{Pm_n} = \varepsilon_n \tag{2}$$

where

$$Q_{in} = \frac{1}{\tau} \int_{t_1}^{t_2} q_{in}\, dt; \quad Q_{nj} = \frac{1}{\tau} \int_{t_1}^{t_2} q_{nj}\, dt \tag{3}$$

and

$$\frac{1}{\tau} \int_{t_1}^{t_2} S_n \frac{dh_n}{dt}\, dt = 0; \quad h_n|_{t_1} = h_n|_{t_2} \tag{4}$$

Q_{in}, Q_{nj} and $\overline{Pm_n}$ denote time-averaged values of the source, discharge and pumping fluxes in cell n, respectively. ε_n is the deviation from water (flux) balance due to various field errors of the fluxes identified entering or leaving cell n.

It is assumed that each cell n within the flow domain and every potential source i of water can be assigned a unique representative concentration, CM_{nk} and C_{ink}, respectively, of a dissolved species (tracer) k. In view of eqns. (2), (3) and (4), the mass balance expression for every tracer $k (k = 1, 2, \ldots K)$ for the time period τ is

$$\sum_{i=1}^{I_n} C_{ink} Q_{in} - CM_{nk} \sum_{j=1}^{J_n} (Q_{nj} + \overline{Pm_n}) = \varepsilon_{nk} \tag{5}$$

where ε_{nk} is the deviation from mass balance associated with tracer k. ε_{nk} expresses sampling and measuring errors associated with the chemical and isotopic analyses of species k in every flow component.

Combining eqns. (2) and (5) into a set of $K + 1$ mass and water balance equations for cell n and upon rearrangement of these expressions into separate known and unknown terms one obtains:

$$\boldsymbol{C}_n \boldsymbol{Q}_n + \boldsymbol{D}_n = \boldsymbol{E}_n \tag{6}$$

where $\boldsymbol{C}$ is a matrix $[(k + 1) \times (I_n + J_n)]$ of known concentrations; $\boldsymbol{D}_n$ is a vector $[(k + 1) \times 1]$ of known flux terms such as rate of pumping or point injection source; $\boldsymbol{E}_n$ is a $[(k + 1) \times 1]$ error vector associated with cell n; and $\boldsymbol{Q}_n$ is a $[(I_n + J_n) \times 1]$ vector of unknown fluxes entering and leaving cell n. A detailed description of the matrix form and the aforementioned vectors is given in Adar and Sorek (1989).

All the flux components in the entire aquifer flow system can now be evaluated by minimizing the sum of the square errors similar to a procedure suggested by Woolhiser et al. (1982).

By virtue of eqn. (6) and by assembling all the square error expressions over all the N cells, one obtains:

$$J = \sum_{n=1}^{N} [\boldsymbol{E}_n^{\mathrm{T}} \boldsymbol{W} \boldsymbol{E}_n] = \sum_{n=1}^{N} [(\boldsymbol{C}_n \boldsymbol{Q}_n + \boldsymbol{D}_n)^{\mathrm{T}} \boldsymbol{W} (\boldsymbol{C}_n \boldsymbol{Q}_n + \boldsymbol{D}_n)] \tag{7}$$

$\boldsymbol{W}$ is a diagonal matrix composed of weighting values for each dissolved constituent. It denotes estimated errors expected for each of the measured terms in the mass balance equations. A comprehensive mathematical description and testing of the computer code with synthetic data including sensitivity analysis are given in Adar et al. (1988).

MODEL IMPLEMENTATION AND RESULTS FROM THE SOUTHERN ARAVA VALLEY

Ground waters of varying chemical and isotopic qualities are exploited by wells drilled in the valley and along its margins. Wells drilled into different blocks and layers showed that due to differences in lithology and mineralogy, each source of recharge provides the alluvial aquifer with water of a specific chemical composition. Also, the isotopic ratios of oxygen-18 to oxygen-16 and deuterium to hydrogen are determined by the geographic location including temperature and the altitude prevailing in the area in which recharge occurs. The spatial isotopic and ionic distribution within the alluvial aquifer along the southern Arava Valley seems to be affected mainly by the relative proportion of recharge contribution from each source. Hence, dilution and mixing are assumed to be the major mechanisms which control the hydrochemical and isotopic composition of the alluvial groundwater reservoir.

The temporal distribution of dissolved ions revealed almost constant concentrations over the last 12 years (Batelaan, 1989). Furthermore, the piezometric head distribution and the pumping regime also seem to be constant for that period (Rosenthal et al., 1990). Hence, changes in heads and concentrations of most species within cell n during time interval τ turned out to be very small and negligible for modeling purposes. This implies an almost steady-state hydrological flow regime, at least for the last decade.

Six ions, TDI, deuterium (D) and oxygen-18 (^{18}O) parameters were finally isolated to characterize every potential source of recharge and to divide the alluvial aquifer into homogeneous compartments. The concentrations which are associated with each potential source flowing into each cell are listed in Table 3. The water samples comprising each cell are listed in Table 2 together with the average ionic concentrations and isotopic ratios. Also in Table 2, the standard deviations for most species are below 5%. As already mentioned before, as a second measure, and to justify the selection of representative wells for each cell, a multivariable cluster analysis was performed considering all wells listed in Table 2. The result is shown in the form of a dendogram in Fig. 2(b). All wells are clustered within significant distinguished groups which support the partitioning of the aquifer into six cells, as presented in Fig. 4.

The potential sources of inflows into each cell, and the associated characteristic concentrations, are also listed in Table 3. The assigned wells, selected on the basis of multivariable factor and cluster analyses (Rosenthal et al., 1990), were found to be the most feasible for representing each of the potential sources of recharge. Rates of pumpage for each cell were obtained from pumping records in production wells since 1965. The yearly average pumpage rates from each cell over the last decade are given in Table 4. Rates of outflow from the last cell (No. 6) into the Gulf of Elat were estimated by Kanfi (1972) to be $0.327 \times 10^6 m^3 year^{-1}$. Since the geometry of the interface with sea water has remained constant for the last decade, it was assumed that the aforementioned discharge is still valid. Discharged (losses) by evapotranspiration in the Elat, Evrona and Yotvata sabhahs was not considered in the overall water balance for the deep alluvial aquifer. Observations have shown that due to high water exploitation, the groundwater table has dropped far below the sabhah's soil surface. Hence, it was assumed that evapotranspiration is of minor importance for the water balance in the alluvial aquifer as compared with the rate of pumping. Optimized solutions for a set of chemical and isotopic mass balance expressions in the form of eqn. (7) were obtained by use of Wolf algorithm for quadratic programming (Wolf, 1967).

Several configurations of cells and potential inflows were modeled. For only four close configurations, the Wolf algorithm solver provided a solution. For the remainder, unbounded solutions or none at all were obtained. Results for four of the best configurations are presented below.

Table 5 presents the result for 17 potential inflows obtained with seven

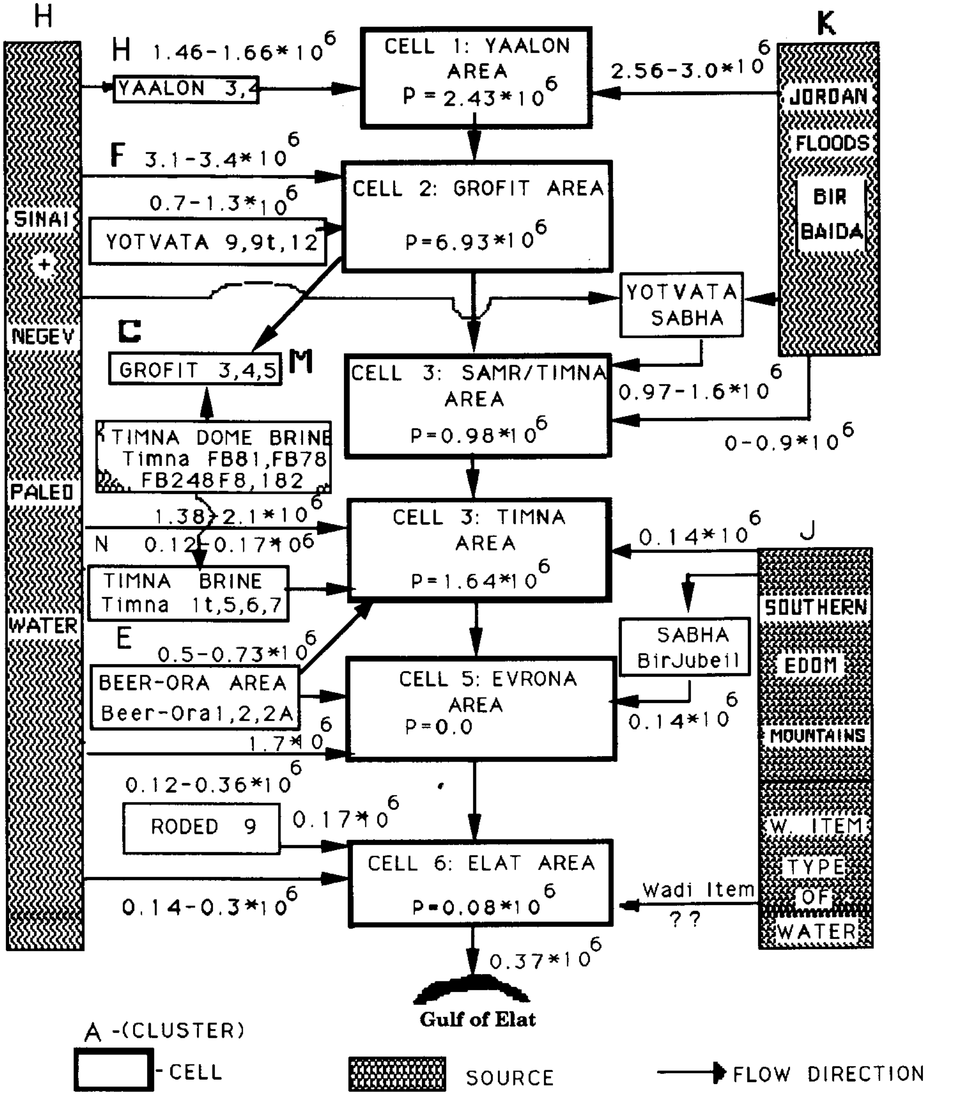

Fig. 4. Schematic modified flow system for the southern Arava Valley with calculated values of recharge.

dissolved ions without isotopes and with a similar weight factor (the values (w) along the diagonal of $\boldsymbol{w}$ equal to 1) for all tracers (flow configuration no. 1). Tables 6, 7 and 8 show the results for only 12 potential inflows for which stable isotope data were available. Table 6 shows results where both oxygen-18 values and dissolved ions were given an equal weight in the concentration matrix (configuration no. 2). Table 7 shows results when deuterium values were also included in the mass balance expressions (configuration

TABLE 4

Average rates of pumpage assigned for the modeled cells

Cell	Volume ($10^3\,m^3$)	Cell	Volume ($10^3\,m^3$)
1	2433.650	2	6930.047
3	978.933	4	1639.217
5	0.000	6	80.733

TABLE 5

Optimized solution for 17 potential inflows based on dissolved chemicals without isotopes (names represent type of water as illustrated in Fig. 4)

Cell	Unknown inflow			
	Name of inflow	Rate of inflow ($10^6\,m^3\,year^{-1}$)	Percentage of total inflow	Percentage of cell inflow
1	BIR BAIDA	2.5594	20.5	56.2
	BAAGEBUL	0.3284	2.6	7.2
	YAALON 3/4	1.6686	13.4	36.6
2	YOTVATA 12	3.4097	27.3	98.1
	YOTVATA 9	0.0671	0.5	1.9
	YOTVATA 9t	0.0000	0.0	0.0
3	BAAGEBUL	0.0918	0.7	8.6
	YOTVATA 9	0.9710	7.8	91.4
4	YOTVATA 9t	1.3776	11.0	57.3
	BEER ORA 1	0.726	5.8	30.2
	BIR JUBEIL	0.1353	1.1	5.6
	TIMNA 6	0.1670	1.3	6.9
5	BEER ORA 1	0.3556	2.9	53.2
	BIR JUBEIL	0.1461	1.2	21.9
6	RODED 9	0.1669	1.3	54.6
	YAALON 3	0.1388	1.1	45.4

Total estimated inflows: $12.4763 \times 10^6\,m^3\,year^{-1}$ (100.0%).
Q_{out} + total pumpage: $12.4307 \times 10^6\,m^3\,year^{-1}$; absolute difference: 0.0456 (0.3668%).
Total salt output: 72174.2 kg year^{-1}; total estimated input: 77117.0 kg year^{-1}.
Percent difference: 6.85%.

TABLE 6

Results for 12 potential inflows based on ions and oxygen-18 (names represent type of water as illustrated in Fig. 4)

Cell	Unknown inflow			
	Name of inflow	Rate of inflow ($10^6\,m^3\,year^{-1}$)	Percentage of total inflow	Percentage of cell inflow
1	BIR BAIDA	2.3640	18.8	61.7
	YAALON 3/4	1.4656	11.7	38.3
2	YOTVATA 9t	0.4836	3.8	11.5
	YOTVATA 12	3.4289	27.3	81.4
	YOTVATA 9	0.2993	2.4	7.1
3	YOTVATA 9t	1.2757	10.2	100.0
4	YOTVATA 9t	2.1465	17.1	76.2
	BEER ORA 1	0.5225	4.2	18.6
	TIMNA 6	0.1476	1.2	5.2
5	BEER ORA 1	0.0000	0.0	0.0
	YAALON 3	0.1265	1.0	100.0
6	YAALON 3	0.3026	2.4	100.0

Total estimated inflows: 12.5628 × $10^6\,m^3\,year^{-1}$ (100.0%).
Q_{out} + total pumpage: 12.4307 × $10^6\,m^3\,year^{-1}$; absolute difference: 0.1321 (1.0627%).
Total salt output: 71960.7 kg year^{-1}; total estimated input: 71635.7 kg year^{-1}.
Percent difference: −0.45%.

no. 3). Table 8 presents the results for the same configuration as in Table 7, but with a preferential weighting factor ($w = 1$) for conservative tracers such as oxygen-18 and deuterium, and reduced weight ($w = 0.5$) for the dissolved ions (configuration no. 4). The number of eastern potential sources (Transjordan) was limited due to lack of isotopic analyses. In all four runs water balance errors were very low (1% or smaller). The difference in the calculated recharge component into cell 1 from the Edom mountains (represented by Bir Baida and Baagebull) as evaluated without isotopes (Table 5), and with isotopes (Tables 6–8) is less than 5%. Hence the lack of Baagebull sample from the three configurations with isotopic data should not greatly affect the overall water balance. The errors associated with the optimization of mass balance equations of dissolved ions, varies from 0.45% in configuration no. 2 up to 6.85% in configuration no. 1. It is important to notice, however, that the deviation of fluxes between assessed inflows and the assigned outflows are heavily dependent on the assigned rates to the known outflows. The absolute

TABLE 7

Results for 12 unknown inflows based on seven ions and oxygen-18 and deuterium (names represent type of water as illustrated in Fig. 4)

Cell	Unknown inflow			
	Name of inflow	Rate of inflow ($10^6\,m^3\,year^{-1}$)	Percentage of total inflow	Percentage of cell inflow
1	BIR BAIDA	2.7461	21.9	82.9
	YAALON 3/4	0.5665	4.5	17.1
2	YOTVATA 9t	1.3672	10.9	30.6
	YOTVATA 12	3.1022	24.7	69.4
	YOTVATA 9	0.0000	0.0	0.0
3	YOTVATA 9t	1.6230	12.9	100.0
4	YOTVATA 9t	2.0732	16.5	76.1
	BEER ORA 1	0.5044	4.0	18.5
	TIMNA 6	0.1453	1.2	5.3
5	BEER ORA 1	0.0198	0.2	14.0
	YAALON 3	0.1215	1.0	86.0
6	YAALON 3	0.2668	2.1	100.0

Total estimated inflows: $12.5360 \times 10^6\,m^3\,year^{-1}$ (100.0%).
Q_{out} + total pumpage: $12.4307 \times 10^6\,m^3\,year^{-1}$; absolute difference: 0.1053 (0.8471%).
Total salt output: 70607.8 kg year^{-1}; total estimated input: 69303.4 kg year^{-1}.
Percent difference: -1.85%.

values of these deviations have no real meaning aside from the fact that for more reliable flow configurations one may expect to obtain lower deviations.

The total groundwater recharge in the four configurations varies between 12.48×10^6 and $12.56 \times 10^6\,m^3\,year^{-1}$, with an average of $12.52 \times 10^6\,m^3\,year^{-1}$ and standard deviation of $0.04 \times 10^6\,m^3\,year^{-1}$. The Nubian sandstone aquifer (as indicated by water samples from wells such as Yaalon 3/4, 3-65, Yotvata 9-55, 9 and 12) underlying the alluvial formations is the major source of the recharge to the alluvial aquifer. The contribution of the Nubian sandstone water is: (1) 64.0%; (2) 75.9%; (3) 72.9%; and (4) 69.4% of the total recharge in the four configurations, respectively. It is evident that the elimination of two potential contributors from the Transjordan sandstone formations in the last three configurations (due to lack of stable isotope data) was compensated for by an increase in the fluxes coming out of the Nubian sandstone which have similar chemical and isotopic compositions.

Water balances for each cell show consistent negative estimated net inflows

TABLE 8

Results obtained for 12 unknowns with weight factor $w = 1$ for oxygen-18 and deuterium and $w = 0.5$ for ions (names represent type of water as illustrated in Fig. 4)

Cell	Unknown inflow			
	Name of inflow	Rate of inflow ($10^6\ m^3\ year^{-1}$)	Percentage of total inflow	Percentage of cell inflow
1	BIR BAIDA	3.0131	24.1	100.0
	YAALON 3/4	0.0000	0.0	0.0
2	YOTVATA 9t	1.7687	14.2	35.5
	YOTVATA 12	2.7656	22.2	55.5
	YOTVATA 9	0.4490	3.6	9.0
3	YOTVATA 9t	1.6349	13.1	100.0
4	YOTVATA 9t	1.7297	13.9	72.9
	BEER ORA 1	0.5245	4.2	22.1
	TIMNA 6	0.1183	0.9	5.0
5	BEER ORA 1	0.1788	1.4	70.0
	YAALON 3	0.0765	0.6	30.0
6	YAALON 3	0.2220	1.8	100.0

Total estimated inflows: $12.4811 \times 10^6\ m^3\ year^{-1}$ (100.0%).
Q_{out} + total pumpage: $12.4307 \times 10^6\ m^3\ year^{-1}$; absolute difference: 0.0504 (0.4054%).
Total salt output: $70607.8\ kg\ year^{-1}$; total estimated input: $68408.3\ kg\ year^{-1}$.
Percent difference: -3.12%.

for cells 2 and 3. (In configuration no. 3, a slight negative balance was also observed in cell 4.) Since pumping rates are well-known measured values, it means that in these cells the pumping rate exceeds the rate of recharge. The maximum estimated over-pumpage in the Yotvata–Grofit area, which is known to be the major well field in the southern Arava, is $1.6 \times 10^6\ m^3\ year^{-1}$.

Models with dissolved ions only (configuration no. 1) and then with ions and isotopes (configuration no. 2; Tables 5 and 6, respectively) correspond very well with each other regarding the estmated rates of inflows. Both runs assign about 20% of the total recharge to cell 1, (from Bir Baida, an eastern alluvial fan). The first two cells comprise more than 60% of the total recharge, while the southern cells (5 and 6) receive less than 8% of the total recharge. This is probably a result of an increase in aridity, as well as smaller tributaries joining the last sections of the southern Arava Valley.

Results of the simulation with ions, oxygen-18 and deuterium (Table 8) are very similar to the previous two, except for the contribution from the Nubian sandstone aquifer (Yaalon 3/4) in cell 1, which is significantly lower. However, this is compensated for by a higher contribution of Yotvata 9T (also Nubian water) into cell 2. This is further supported by the results from the fourth configuration where oxygen-18 and deuterium were given higher weights ($w = 1$), while ions were assigned only half ($w = 0.5$).

SUMMARY AND CONCLUSIONS

This paper demonstrates that environmental tracers can be used to identify the hydrogeological pattern and to provide quantitative assessment of the subsurface flow system of an arid basin with an extremely complex geology. The numerical modeling based on the flow equation could not be implemented due to the lack of hydrological parameters, the existence of multiple water-bearing layers, and hence, complex boundary conditions. In the first step hydrochemical and isotopic data were statistically processed by multivariable cluster analyses to identify different water bodies and potential sources of recharge. Later the same data were processed by quadratic programming, utilizing the Wolf algorithm (1967), to provide a reliable and unique solution for unknown recharge components although other optimization techniques should be applicable as well. This paper shows the possibility of utilizing environmental tracers for quantitative assessment of recharge and the groundwater flow system in an alluvial arid basin with scarce hydrogeologic data.

The calculated recharge is a sum of lateral inflows and upward leakage into every section along the southern Arava Valley. Other recharge processes, such as direct infiltration from floods, play a minor and, hence, negligible role as floods seldom reach the lower southern Arava Valley. Most floods infiltrate along tributaries and over the alluvial fans before they reach the lower valley. Only extreme floods flow short distances into the sabhahs where they eventually evaporate. The four most feasible configurations of the optimization scheme revealed that the total recharge is around $12.52 \times 10^6\,m^3\,year^{-1}$ (with a small standard deviation of $0.04 \times 10^6\,m^3\,year^{-1}$), where the uppermost section (cells 1 and 2) receives about 64% of the total recharge. From 60 to 80% of the recharge into the uppermost basin (cell 1) originates over the eastern Edom mountains. Although it is only about 24% of the total inflow, the latter is the major source for fresh water (not brackish) flowing into the southern Arava basin. Also, it appears that the well field near Yotvata–Grofit (cell 2) is heavily exploited with over-pumping of $1.6 \times 10^6\,m^3\,year^{-1}$. The range of computed values of recharge from the four configurations is listed in Fig. 4. Some of the differences are due to the lack of isotopic information for some of the Jordanian potential contributors. The flow configuration into the modeled aquifer is slightly different from that previously suggested by the authors (fig. 8, Rosenthal et al., 1990). Some of the potential sources that had been introduced into the model and came out with significant zero inflows, were omitted from the final flow model as presented in Fig. 4.

Small differences between the four runs indicate relative stability of the quadratic simulation within the reliable domain of the solution. For a flow system with a rather different flow configuration, the quadratic programming solver indicated an unbounded flow system and no solution could be reached.

Experience has shown (Adar and Neuman, 1988; Adar et al., 1988) that a solution for such a model can be obtained only for a well-posed hydrogeological, chemical and isotopic system. In the case of a wrong allocation for the potential inflows and assigning wrong characteristic isotopic and chemical concentrations, a quadratic optimizing scheme such as the Wolf algorithm does not lead to a unique optimal solution. Hence, it seems that quantitative assessment of inflows is very sensitive to reliable input data such as a realistic flow system and accurate concentrations. Even a slight modification of one significant potential inflow may cause a badly posed unbounded solution. On the other hand, misinterpretation of a non-significant contributor that is isotopically and chemically similar to another potential source, will not change the final assessment of the recharge components significantly. The flux that should be assigned to the less dominant flow component will be attached to the most significant and pronounced source with similar chemical and isotopic characteristics. The way the objective function was set, though water and the mass balance expressions were written for each compartment separately, the solution is obtained simultaneously for the entire flow domain. This procedure ensures that local errors are not spread over the whole cells and can be identified right away.

REFERENCES

Adar, E.M. and Neuman, S.P., 1988. Estimation of spatial recharge using environmental isotopes and hydrochemical data, II. Application to Aravaipa Valley in southern Arizona, USA. J. Hydrol., 97: 279–302.

Adar, E.M. and Sorek, S., 1989. Multi-compartmental modelling for aquifer parameter estimation using natural tracers in non-steady flow. Adv. Water Resour., 12(2): 84–89.

Adar, E.M., Neuman, S.P. and Woolhiser, D., 1988. Estimation of spatial recharge using environmental isotopes and hydrochemical data, I. Mathematical model and application to synthetic data. J. Hydrol., 97: 251–277.

Batelaan, O., 1989. Qualitative and quantitative recharge study of the southern Arava Valley, Israel. M.Sc. Thesis, Department of Hydrogeology, Institute of Earth Sciences, 107 pp.

Campana, M.F. and Simpson, E.S., 1984. Groundwater residence times and recharge rates using discrete-rate compartment model and ^{14}C data. J. Hydrol., 72: 171–185.

Everit, B.S., 1980. Cluster Analysis, 2nd edn. Heineman Educational, London, 136 pp.

Kanfi, Y., 1972. The hydrology of groundwater in southern Arava and its influence on the geochemistry of the water. M.Sc. Thesis, Hebrew University, Jerusalem, 55 pp (in Hebrew).
Kirk, S.T. and Campana, M.E., 1990. A deuterium-calibrated groundwater flow model of a regional carbonate-alluvial system. J. Hydrol., 119: 357–388.
Norusis, M.J., 1985. SPSS Advances-Statistical Guide. McGraw Hill and SPSS Inc., Chicago, IL.
Rosenthal, E., Adar, E., Issar, A.S. and Batelaan, O., 1990. Definition of groundwater flow pattern by environmental tracers in the multiple aquifer system of Southern Arava Valley, Israel. J. Hydrol., 117: 339–368.
Simpson, E.S. and Duckstein, L., 1976. Finite state mixing-cell models. In: V. Yevjevich (Editor), Karst Hydrology and Water Resources, Vol. 2. Water Resource, Ft. Collins, CO, pp. 489–508.
Wolf, P., 1967. Methods of Non-linear Programming. In: J.J. Abadie (Editor), Interscience, Chapter 6, Wiley, New York, 97–131.
Woolhiser, D.A., Gardner, H.R. and Olsen, S.R., 1982. Estimation of multiple inflows to a stream reach using water chemistry data. Trans. ASAE, 25(3): 616–622.